

Shallow Water Surface Gravity Wave Imaging, Spectra and Their Use in Shallow Water Dredging Operations

Charles R. Bostater Jr. *, Bingyu Yang

Marine Environmental Optics Laboratory and Remote Sensing Center, College of Engineering,
Florida Institute of Technology, 150 West University Blvd., Melbourne, Florida, USA 32901

ABSTRACT

Imaging of shallow waters using high resolution video imagery is described. Common to mono, stereo and trinocular imaging approaches from ground and airborne platforms is the need to validate the surface water wave field measurements, particularly the amplitude and specular reflectance of water surface small gravity waves. A technique for calibration and validation of water surface gravity wave field energy spectra is described. Results demonstrate the value of video imagery where water level staff gauges with approximately with 0.5 cm wave height accuracy are easily sensed using high definition videography. Essentially, a staff gauge placed in shallow water constructed from PVC materials with custom colored line coding are imaged at 30 H or high frame rates, followed by frame by frame analyses in order to detect the water level measured at 0.5 cm height intervals. The image based time series allow the development of shallow water gravity wave energy spectra using standard FFT analysis procedures. Spectral models based upon peak frequency, for example, are then used in a two dimensional water surface wave simulation model that generates radiative transfer based hyperspectral images of the water surface wave field. The simulated and observed water surface wave patch fields are compared by extracting vertical or horizontal transects within observed and simulated imagery. The approach allows one to developed spectral energy model probability distributions at low cost. The novel noncontact video sensing and image analysis methodology used to calibrate and validate shallow water gravity wave models yield a means for ultimately calculating bottom boundary velocities under measured or simulated wave fields. These boundary layer velocities can cause migration and horizontal particle fluxes ($\text{g cm}^{-2} \text{s}^{-1}$), resuspension, settling, and increased turbidity during dredging operations, but not necessarily due to waterway dredging operations and activities.

Key Words: hyperspectral sensing, surface wave imaging, gravity waves, spectral models, radiative transfer modeling, Monte Carlo modeling, shallow water sensing, particle resuspension, turbidity, video imaging, airborne remote sensing, multi-angle imaging, dredging, fluid mud, muck, noncontact sensing, video analysis, subsurface probes, estuaries

1. INTRODUCTION

Background

Existing airborne, ship, in-situ and shoreline based sensing platforms using multispectral and hyperspectral sensing single and multi-sensors (stereo, trinocular) make observations at nadir and multiple angles. Existing airborne and satellite imagers such as MISR and AirMISR^{1, 2} are commonly known multi-angle imaging systems. Airborne point cloud stereo sensing³ as well as multi-angle spectral signatures⁴ are being used in operational earth remote sensing. The calculation of the bidirectional reflectance distribution function (BRDF)⁵ and the bidirectional reflectance factor (BRF)⁶ have been accomplished using airborne and satellite platforms as well as ground based multi-angle sensing platforms⁷ and from vessels^{8, 9}. Existing airborne and future satellite missions with small ground sampling distances (GSD) such as AirSWOT and SWOT may provide unparalleled noncontact water surface wave imaging for small shallow water regions using K_a band sensing and interferometry^{10, 11}. Bostater, et al.^{8, 9, 12, 13} have used not only twin airborne platforms, but also ground and fixed sensing platforms and related multi-angle goniometer systems to make BRDF and BRF based anisotropic factors. These factors are needed to correct multiangle sensor data in order to help characterize reflectance of the water surface, for example of weather oil on the water surface and in vegetative dysfunction monitoring.

*cbostate@fit.edu, Florida Institute of Technology, Marine Environmental Optics Lab & Remote Sensing Center, College of Engineering, 150 West University Blvd., Melbourne, Florida 32901, ph. 321-258-9134

To date, there is a paucity of reports regarding investigations of anisotropic factors for surface water gravity wave imaging using mono, stereo and trinocular sensing methods, however each of these later techniques require ground truth validation for calibration and development of spectral energy models of shallow water surface gravity wave fields. The methods described below describe videography using modern high definition cameras to sense the water surface small gravity wave field in a shallow water lagoon along the eastern Atlantic Ocean, near Melbourne, Florida as shown in Figure 1 below.

2. TECHNIQUES & METHODS

2.1 Video Sensing System for Spectral Water Wave Model Technique Development



Figure 1. Location of the research area and in-situ video imaging of the water surface gravity wave field (left) located in the Space Coast Florida region (left) near a proposed dredging area. A water surface patch 4.5 m² area in shallow water (< 1 m depth) with in-situ staff gauges for capillary small gravity wave imaging, spectral water wave model research, water wave imaging model validation.

As depicted above, *in-situ* staff gauges are deployed in shallow waters. A rectangular region bounds the an imaging area of interest where mono, stereo or trinocular measurements. During the measurements described below, stereo and mono video acquisition sequences were collected during 2014. The sensor systems were mounted on a rotatable goniometer type tripod for fixed or variable rotation. Each *in-situ* staff gauge is custom replicated and mounted (inserted) within the bottom sediments. The gauges are coated with a 2 color – 0.5 cm spacing horizontal line structure as shown in Figure 2.

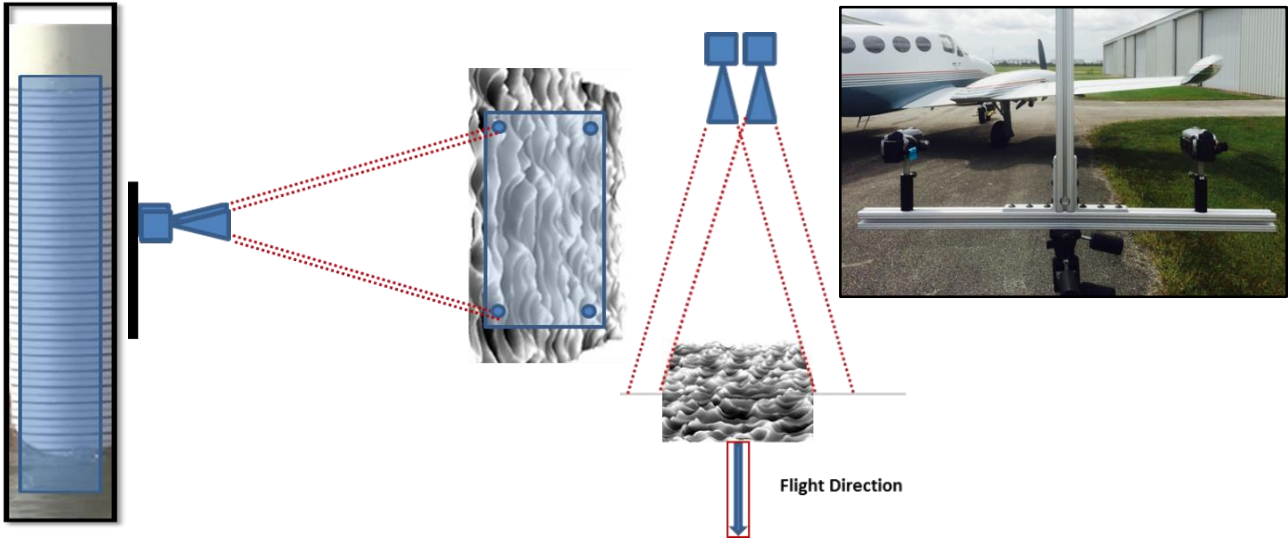


Figure 2. (left) *In-situ* bottom mounted staff gauge with color coded lines (0.5 cm spacing) sensed at 30 HZ using dual video cameras with zoom & linear polarizer lens capability. A wave patch is imaged as depicted (center) using 2 time synchronized video cameras for bidirectional reflectance factor (BRF) calculations. A dual video sensor configuration is also flown on a twin engine airborne platform depicted (right) with a hyperspectral imager (~2-5 cm GSD, 1034 pixel swath & 1024 bands) and a photogrammetric 9 inch frame camera with similar GSD for obtaining high resolution digitally scanned aerial images (~255 megapixels) of the water surface.

The steps to process an *in-situ* staff gauge video sequence of the surface gravity wave field is given below along with an example of the analysis of one video frame taken with a 30 HZ frame rate from one of the 4 staff gauges. Earlier research conducted regarding the imaging process demonstrated that the novel technique is nearly identical or independent of the channel (R,G,B) used from the high definition video camera that utilizes high sensitivity gain, low light level and xoomed focusing during a video sequence recording.

Video sequence sensor recordings can be made with or without embedding the sound or an acoustic field sensor at or near the shallow water surface using the cameras (with or without external microphones). Research is underway to utilize the wind acoustic field to estimate the wind velocity and direction in shallow waters at or near the video cameras^{14, 15}.

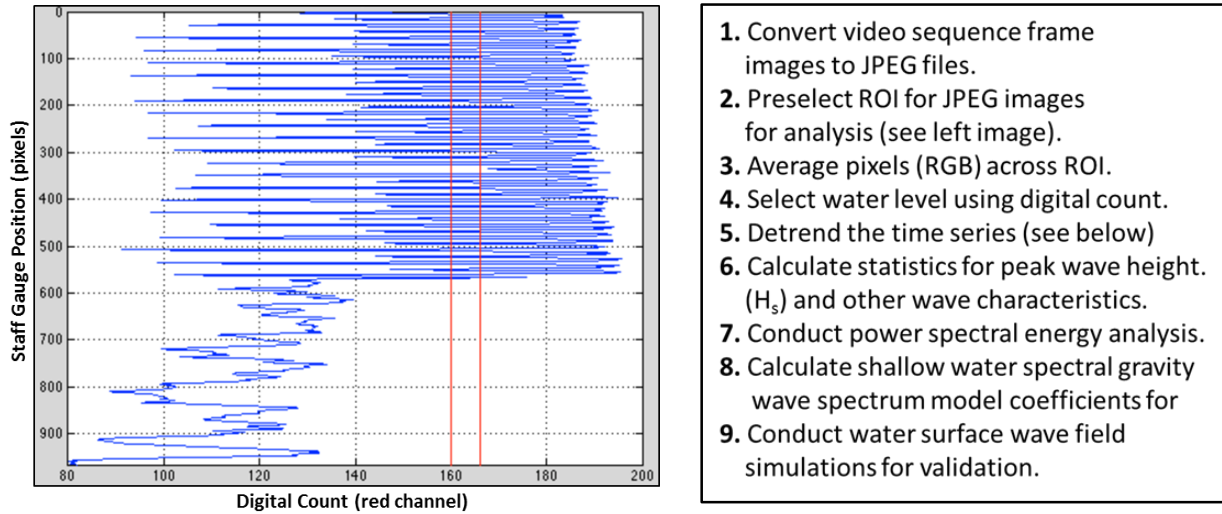


Figure 3. Image analysis and procedures of video frames acquired from the staff gauge imaging is composed of 9 steps. An example analysis result (left) of a video frame image showing the obvious position (in pixels) of the water surface on the calibrated staff gauge.

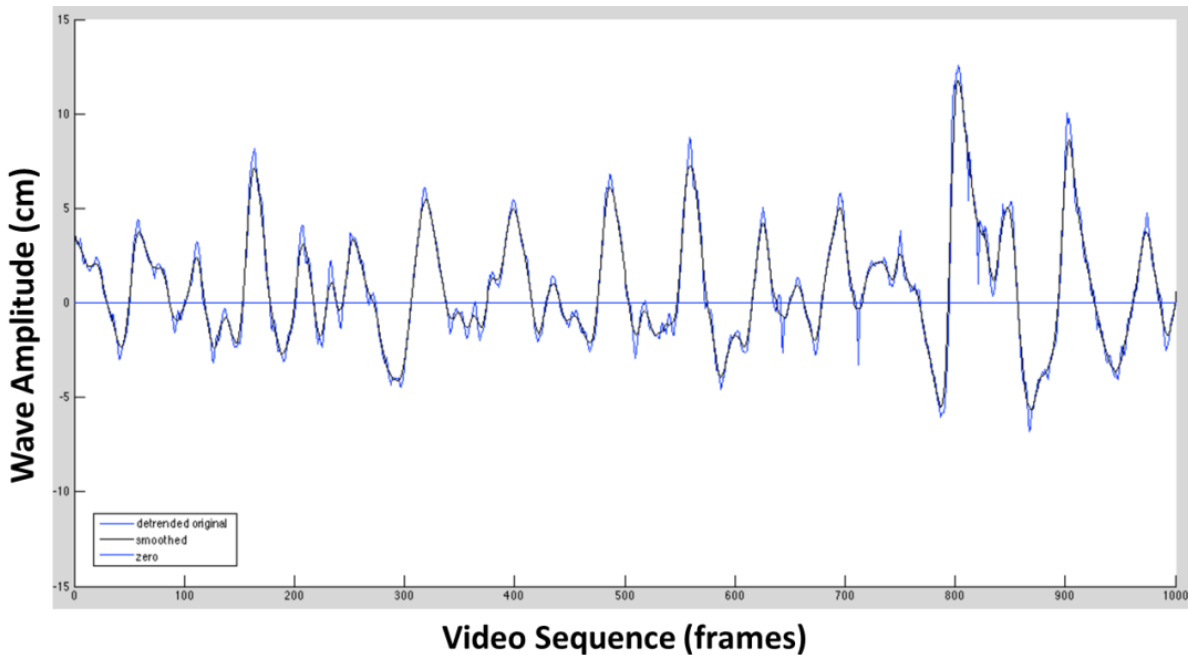


Figure 4. Example detrended video sequence collected at 30 HZ showing wave heights (wave amplitude) in cm for 1000 frames where each frame was analyzed using the technique described and shown above. Smoothed and original data using the 0.5 cm line calibration spacing are shown.

2.2 Bottom Boundary Layer Probes and Near Bottom Reflectance Targets

The wave heights and power spectrums can be used for estimating the bottom boundary layer orbital velocities¹⁶ and vorticity dynamics responsible for resuspension of fluid mud or muck. This shear strain resuspension process causes changes in water depth and increased turbidity due to vertical and horizontal movement of the fluidized muck. Measurement of mass of this non-Newtonian material in terms of its fluidized movement (migration) in the bottom frictional layer due to small gravity waves is first achieved by using measurement probes along with subsurface imaging designed for horizontal and vertical flux ($\text{gm cm}^{-2} \text{sec}^{-1}$) measurements. Reduction in the fluid mud mass flux (movement) is desirable in environmental quality related dredging.

Figure 5 shows several probes developed for estimating the flux of the bottom sediment and fluidized mud (muck) in terms of $\text{gm cm}^{-2} \text{sec}^{-1}$. The horizontal flux probes (top 4 images below) can be placed just above the water bottom and measure the horizontal particle flux in selected directions. The upper right images were taken when the probes were submerged. The flat panel probe is specially constructed so the edge areas trap and thus allow one to measure the flux at perpendicular flux directions. The inner white panel is specially constructed using a calibrated reflectance coating for subsurface hyperspectral imaging of the fluidized mud deposits upon the reflectance panel. The lower center and right images show upwards and downward probes for suspending at specified depths within a water column. All probes provide flux reported as wet and dry weight ($\text{gm cm}^{-2} \text{sec}^{-1}$). Washing of the dried material using deionized water allows the measurements to be corrected for the presence of the water salt concentration during a deployment period.

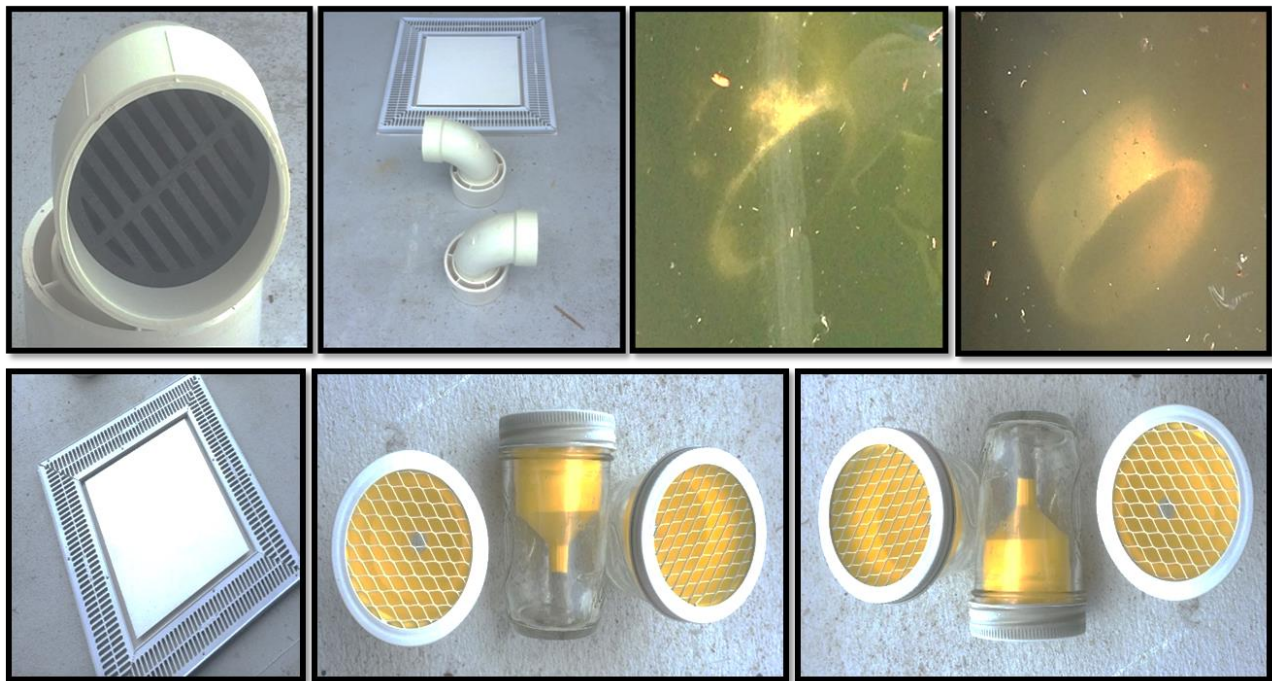


Figure 5. (upper) Horizontal bottom boundary layer fluid mud and floc particle probes used to measure the flux (movement) of near bottom material ($\text{g cm}^{-2} \text{sec}^{-1}$) in shallow water aquatic environments. The white panel probe provides flux measurements in addition to hyperspectral imaging of the bottom material moving over the white calibrated bottom reflectance panel. Probes (lower center and right) are also suspended in the water column for trapping settled and resuspended particle flux.

The above probes provides a means to calibrate and validate the predicted mass flux due to shallow water small gravity waves upon water quality due to wave induced fluid mud migration and associated suspended or settled particles and estuarine flocs. These measurements are made in the vicinity of staff gauges.

2.3 Surface Water Gravity Wave Simulation and Modeling Methods

Surface water gravity wave spectral model coefficients for shallow water environments such as Banana River and Indian River Lagoon obtained from the image processing of the video image sequences are used to calculate probability based waves model. The spectral models are then used as input to a FORTRAN 90 radiative transfer simulation program developed and described by Bostater, et al.^{17, 18, 19}. The spectral wave models are used to simulate the water surface gravity wave fields as shown below.

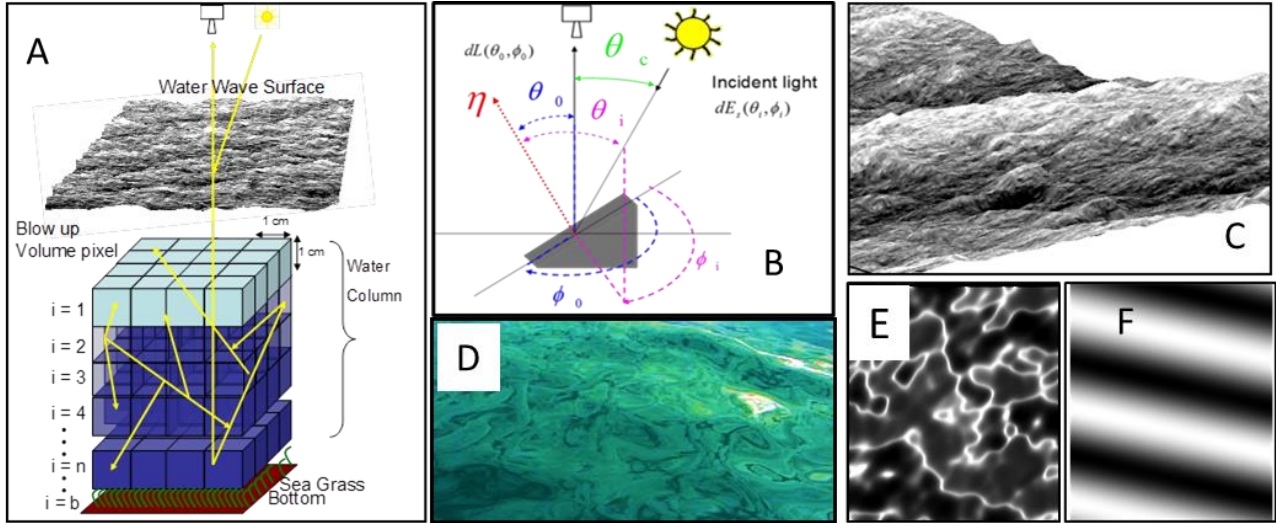


Figure 6. Conceptual schematic (a) showing the FORTRAN 90 hyperspectral Monte Carlo model^{17,18,19} approach wherein numerically tagged photons enter a simulated water surface facet (b) obtained from simulating a shallow water small gravity wave field depicted in (c). Video images such as (d) are used to create the small gravity wave model coefficients. The gravity wave models are developed, calibrated and validated using the measured video imaging of a wave field patch. Figure (e) shows an example 2 dimensional wave slope facet field at nadir viewing geometry. Spectral gravity wave model coefficients can be adjusted to model uniform wave height fields as demonstrated in (f) and realistic random wave height fields as demonstrated in (c) depending upon the magnitude of the gravity wave model coefficients. These fields are used to validate significant wave height (H_s) characteristics between actual video and simulated wave patches described below.

3. RESULTS

3.1 Shallow Water Wave Model Coefficients for Banana River Location

Shallow water wave fields were simulated using the spectral wave models developed with 2 parameters that allow characterization of the wave height fields and wave facet field. The 2 parameter model fit to the spectral energy FFT in order that wave frequency can be used to simulate the wave height field. An example water surface height field with $\alpha = 2.0$ and $\beta = 1.5$ is shown in Figure 7(a) where the simulated wave patch is 4.5 m^2 using 1024×1024 pixels, where each pixel on the height field for the slope facets are approx. 0.45 cm^2 . The Significant wave height for this example image (H_s) is 0.44 m based upon extraction and analysis of transects from the simulated height field image. Thus, the image corresponds to a wave field patch similar to that shown in Figure 1. Figure 7(b) is an example of a 4.5 m^2 wave patch simulation showing the 2D wave slope facets with spectral wave model coefficients of $\alpha = 4$ and $\beta = 2$

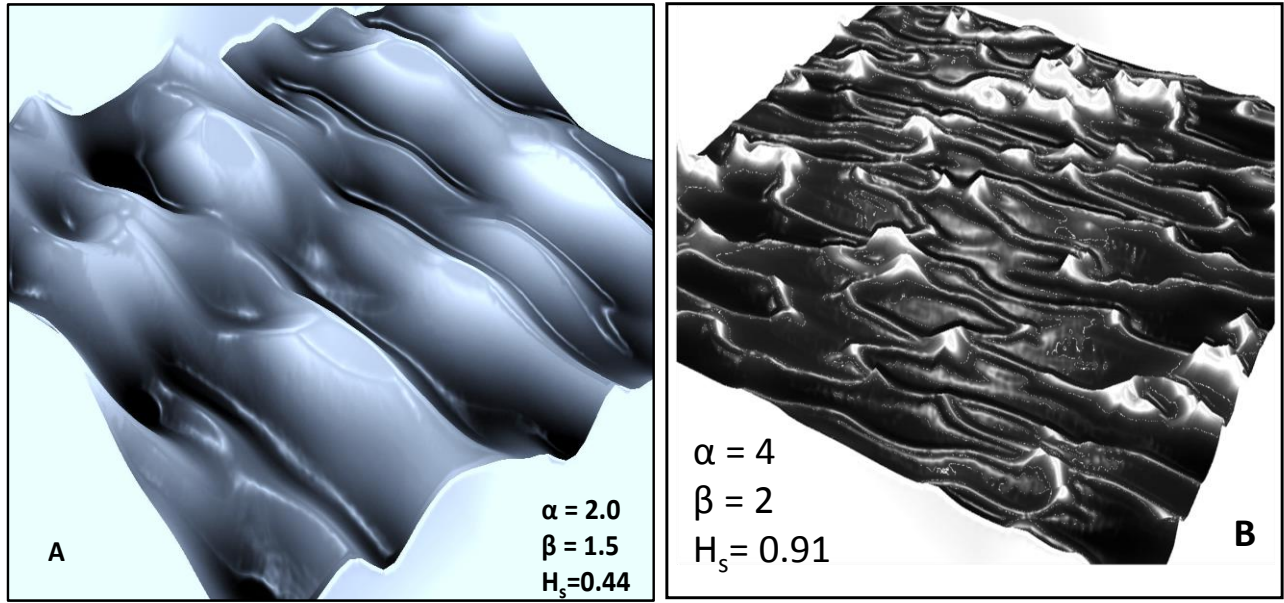


Figure 7. Examples of model outputs. A rendered wave height field patch simulation (a) and an example wave facet field simulation showing rendered specular points from the two dimensional wave facet slope field (b) using a 2 parameter multivariable spectral wave model.

The above wave fields were simulated using a Weibull based distribution as a simple model for mathematical expression of an energy spectrum. The Weibull probability density function (PDF) and the conservation of probability $f(y)$ based cumulative density function (CDF) are expressed as:

$$\text{PDF} - f(y) = \left(\frac{\beta}{\alpha}\right) y^{\beta-1} \exp\left(-\left(\frac{y}{\alpha}\right)^{\beta}\right) \quad y > 0 \quad , \quad (3.1.1)$$

$$\text{CDF} - f(y) = 1 - \exp\left(-\left(\frac{y}{\alpha}\right)^{\beta}\right) \quad y > 0 \quad , \quad (3.1.2)$$

where a is typically called scale parameters and b is called the shape parameter. These parameters are estimated from video sequences of small gravity surface waves in the Indian River Lagoon (including the Banana River) where the parameters are mathematically and dimensionally expressed as a function of: significant wave height (H_s), fetch (L_h), shallow water depth (h_w), wind direction (w_d), wind speed (w_s). The above formulations for a shallow spectral gravity wave models are explicitly two parameter models, but can be implicitly calculated as a function of the above variables through (a) carefully designed field experiments along transects in the Indian River Lagoon and Banana River shallow waters and (b) analysis of wave field “patch simulations” shown in Figures 6 and 7 above.

The two parameters hold a unique value in that they are easily estimated for a variety of density function shapes and are quite easily estimated from statistical FFT based power spectrums derived from optically sensed gravity wave field characteristics. Analysis of the gravity wave patch simulations provide wave height and wavelength based spectrums for model calibration and validation to different shallow waters along a changing bathymetric profile. Additional details concerning the wave simulation procedures for any spectral wave model has been published by Bostater, et al. ^{17, 18, 19}. Excellent additional reviews on water wave simulation techniques and methods have been published in course notes²⁰ and imaging and computer science publications ^{21, 22}.

3.2 Operational Mission Planning Considerations

Application of the methods and techniques during proposed dredging operations involves the following sequence of operations:

Step (1) site selection for staff gauge placements. This coincides with simultaneous selection of transects across a waterway and/or area to be dredged. Placement of staff gauges are arranged in order image a 4 to 10 m² wave patches across transects from shallow to deeper waters. The resulting data allows estimation of near field parameters - α and β as a function of physical and meteorological conditions - including H_s , ξ_h , h_w , w_d , w_s .

Step (2) involves the analysis of video sequences, and calibration, testing and validation of the gravity wave spectral model coefficients.

Step (3) of the methodology involves analysis of the wave patch physical and metrological data to be used in step 2 and simulation of wave patch gravity wave fields.

Step (4) includes simulation of the near bottom water velocity fields and calculation of resuspension and settling of fluid mud and muck for estimation of pre-dredge fluid mud flux and post dredging fluid mud flux. Reduction of moving material from the measured fluxes ($\text{g cm}^{-2} \text{sec}^{-1}$) are thus possible.

An image of typical flocs and fluid mud material obtained from the horizontal probes shown in Figure 5 (top) is shown below.



Figure 8. Example of the fluid mud obtained from horizontal fluid flux probes shown in figure 5 above during a 12 hour deployment in Indian River Lagoon during 2014, for comparison to predicted particle migration from surface and subsurface water wave simulations.

4. SUMMARY AND CONCLUSIONS

The purpose of this paper has been to report on the development of an approach and acquisition of *in-situ* measurements of surface gravity wave modeling to support monitoring in preparation for dredging activities in shallow waters. The techniques are applicable for post dredging monitoring in order to quantify reduction of fluid mud and near bottom muck fluxes ($\text{g cm}^{-2} \text{sec}^{-1}$) during and after dredging.

A new technique to monitor surface gravity waves using video imaging of wave patches with specially designed staff gauges for shallow water aquatic environments is described and demonstrated. This new technique allows for inexpensive measurement and estimation of peak wave heights (H_s).

Estimation of specular point distributions for characterizing wave conditions during dredging from airborne imaging sensors will provide for estimation of bottom boundary layer velocity modeling and related resuspension and settling of the fluid mud and muck.

The predicted bottom fluxes can be related to *in-situ* near bottom flocs and particle flux ($\text{g cm}^{-2} \text{ s}^{-1}$) using new probes described in this paper. The wave patch measurement techniques and related fluid mud (muck) probes represents new techniques that has not been reported before. The video imaging of the novel staff gauge design allows the estimation of small gravity waves \bar{O} ($\sim 1\text{cm}$ height) with far greater ease for placement in shallow waters of varying water depth and fetch characteristics. The low cost of the optical video imaging techniques allows the analysis of high resolution water height levels at many locations simultaneously.

The low cost staff gauge video analysis techniques and *in-situ* probes represent new instruments for improving our scientific understanding of surface gravity waves, associated spectral energy model developments and bottom particle fluxes needed for many engineering and environmental applications.

The techniques should be of value for use in developing spectral wave models in small shallow water bodies as new airborne (AirSWOT) and satellites such as SWOT²⁴ utilize K_a band sensors and interferometry for measuring littoral water surface characteristics.

5. ACKNOWLEDGEMENTS

Funding for this research has been supported by KB Science, Northrop Grumman Corp., Link Foundation, the National Science Foundation, US Dept. of Energy, NASA, the US-Canadian Fulbright Program, and the US Department of Education, *FIPSE* & European Union's grant *Atlantis STARS (Sensing Technology and Robotics Systems)*.

6. REFERENCES

- [1] Diner, D., et al, "The Airborne Multi-angle Imaging SpectroRadiometer (AirMISR): Instrument Description and First Results", IEEE Transactions Geoscience Remote Sensing, IEEE Vol. 36, No. 4, pp. 1339-1349, (1998),
- [2] Lyapustin, A., et al., "Local analysis of MISR surface BRDF and albedo over GSFC and AERONET sites", IEEE Transactions Geoscience Remote Sensing, IEEE Vol. 44, No. 7, pp. 1707-1718, (2006).
- [3] Harwin, S., Lucieer, A., "Assessing the Accuracy of Georeferenced Point Clouds Produced via Multi-View Stereopsis from Unmanned Aerial Vehicle (UAV) Imagery", Remote Sensing, Vol. 4, pp. 1573-1599, (2012).
- [4] Diner, D., et al., "New Directions in Earth Observing: Scientific Applications of Multiangle Remote Sensing", Bulletin of the American Meteorological Society, Vol. 80, No. 11, pp. 2209-2228, (1999).
- [5] Liang, S., Strahler, A., "Retrieval of Surface BRDF from Multiangle Remotely Sensed Data", Remote Sensing of Environment, Vol. 50, pp. 18-30, (1994).
- [6] Slater, P., "*Remote Sensing: Optics and Optical Systems*", Addison-Wesley Pub. Co., pp. 1-575, (1980)
- [7] Martonchik, J., "Retrieval of surface directional reflectance properties using ground level multiangle measurements", Remote Sensing of Environment, Vol. 50, pp. 303-316, (1994).
- [8] Bostater, C., Coppin, G., Levaux, F., Jones, J., Frystacky, H., "Mobile Platform Pushbroom Motion Control. Image Corrections and Spectral Band Selection: Examples of Hyperspectral Imagery Using Low Flying Aircraft and Small Vessels in Coastal Littoral Areas", In: Proceedings Robots for Risky Interventions and Environmental Surveillance-Maintenance (RISE-2011), International Advanced, pp. 1-19, (2011).
- [9] Bostater, C., Coppin, G., Levaux, F., "Hyperspectral Remote Sensing – Using Low Flying Aircraft and Small Vessels in Coastal Littoral Areas", In: Remote Sensing- Advanced Techniques and Platforms, Boris Escalante-Ramerez (Ed.), InTech Publishers, ISBN: 978-953-51-0652-4, pp. 269-288, (2012).
- [10] Walsh, E., Vandemark, D., Friehe, C., Burns, S., Khelif, D., Swift, R., Scott, J., "Measuring sea surface mean square slope with a 36-GH scanning radar altimeter, J. Geophysical Research, Vol. 103-C6, pp. 12587-12601, (1998).
- [11] Alsdorf, D., Rodriguez, E., Lettenmaier, D., "Measuring surface water from space", Reviews of Geophysics, Vol. 45, (2007).

- [12] Bostater, C., Jones, J., Frystacky, H., Kovacs, M, Jozsa, O., "Image Analysis for Water Surface and Subsurface Feature Detection in Shallow Waters", SPIE Vol. 7825, pp. 199-215, (2010).
- [13] Bostater, C., Brooks, D., "Operational Multi-Angle Hyperspectral Sensing for Feature Detection", SPIE Vol. 8888, pp. 8880C1-12, (1998).
- [14] Nystuen, J., Selsor, H., "Weather classification using passive acoustic drifters", Journal. Atmospheric and Oceanic Tech., Vol. 14, pp. 656-666, (1997).
- [15] Bass, H., Raspet, R., Messer, J., "Experimental determination of wind speed and direction using a three microphone array", Journal American Acoustical Society, Vol. 97, pp.695-696, (1995).
- [16] Soulsby, R., "Calculating Bottom Orbital Velocity Beneath Waves", Coastal Engineering, Vol. 11, pp. 371-380, (1987).
- [17] Bostater, C., Chiang, G., Huddleston, L., Gimond, M., "Synthetic Image Generation of Shallow Waters Using a Parallelized Hyperspectral Monte Carlo and Analytical Radiative Transfer Model", SPIE Vol. 4880, pp. 102-116, (2002).
- [18] Bostater, C., Huddleston, L., Bassetti, L., "Synthetic Image Generation of Shallow Water Using an Iterative, Layered Radiative Transfer Model with Realistic Water Surface Waves", SPIE Vol. 5233, pp. 253-267, (2004).
- [19] Bostater, C., "Hyperspectral Simulation and Recovery of Submerged Targets in Turbid Waters", SPIE Vol. 5780, pp. 107-127, (2005).
- [20] Tessendorf, J., "Simulating Ocean Water," SIGGRAPH 2001 Course notes, <http://graphics.ucsd.edu/courses/rendering/2005/jdewall/tessendorf.pdf>, pp 1-19, (2001).
- [21] Premoze, S., Ashikhmin, A., "Rendering Natural Waters," In: Eighth Pacific Conference on Computer Graphics and Applications, Hong Kong, 3-5 October, pp.23-30, (2000).
- [22] Mastin, G., Watterger, P., Mareda, J., "Fourier Synthesis of Ocean Scenes", IEEE CG&A, pp. 16-23 (1987),
- [23] Cerezo, E. and Serón F., "Synthetic Images of Underwater Scenes: A First Approximation", In: Proceedings of the 9th International Conference in Central Europe on Computer Graphics and Visualization WSCG'01, pp. 395– 402, (2001).
- [24] Alsdorf, D., Rodriguez, E., Lettenmaier, D., "Measuring surface water from space", Geophysics Reviews, Vol. 45, pp. 1-24, (2007).